Materials Research. 2018; 21(5): e20170860
DOI: http://dx.doi.org/10.1590/1980-5373-MR-2017-0860

High Temperature Tensile and Strain Hardening Behaviour of AA5052/9 vol. %ZrB_2 insitu Composite

Narendra Kumar[a]*, Gaurav Gautam[b], Anita Mohan[c], Sunil Mohan[d]

[a]Department of Mechanical Engineering, Bundelkhand Institute of Engineering & Technology, Jhansi, India
[b]Department of Metallurgical and Materials Engineering, Indian Institute of Technology Roorkee, Uttarakhand, India
[c]Department of Physics, Indian Institute of Technology (BHU), Varanasi, India
[d]Department of Metallurgical Engineering, Centre of Advanced Study, Indian Institute of Technology (BHU), Varanasi, India

Received: September 26, 2017; Revised: June 18, 2018; Accepted: July 23, 2018

Various mechanical components such as piston, cylinder blocks, brakes and drums, have to operate under high temperature condition during their service life. Therefore, to meet the demand of high strength materials, a detailed analysis of their synthesis and high temperature tensile behaviour is of utmost importance. Present study is an effort in this direction to develop AA5052/9vol. %ZrB_2*insitu* composite by salt-metal reaction technique. An *insitu* reaction between molten aluminium alloy and two inorganic salts K_2ZrF_6 and KBF_4 begins at 860°C and continues up to 30 min. The resulting reaction product ZrB_2 is desired reinforcement confirmed by XRD analysis. Microstructural study was performed to analyse grain size, particle morphology, and their distribution in the matrix. Tensile tests were conducted at temperatures ranging from room temperature (RT) to 200°C with an interval of 50ºC. The results revealed the decreasing trend of UTS and YS (0.2% off set) with increase in temperature; however ductility increased with temperature. The composite is able to maintain about 81% of its ambient temperature strength at 150°C and 72% at 200°C. Strain hardening exponent was not significantly affected with temperature and tensile properties were correlated with fractured surface morphology examined under SEM to understand the mechanism.

Keywords: *ZrB_2, high temperature, strain hardening.*

1. Introduction

Particulate aluminium matrix composites (PAMCs) are widely used for manufacturing of various mechanical components such as piston, cylinder brakes, discs/drums and piston insert rings, due to their high strength to weight ratio, good thermal and electrical conductivity, good corrosion and wear resistance characteristics[1,2]. PAMCs are synthesized either by *exsitu* or *insitu* process. *Exsitu* involves the addition of externally synthesized reinforcement particles into the melt, whereas, desired reinforcement particles are formed during melting within melt during *insitu* process. Among these techniques, *insitu* is preferred because it provides uniform distribution of reinforcement particles, finer particles, excellent bonding between particle and matrix, isometric properties, reaction free interface, and enhanced thermodynamic stability of reinforcement with the matrix[3-6]. Therefore, *insitu* composites possess superior properties as compared to *exsitu* composites[7]. PAMCs are generally reinforced with variety of ceramic particles in the form of carbides, oxides, nitrides, and borides[8-11]. Being an ultra-high temperature ceramic and other characteristics such as high melting point, high hardness, high temperature strength, high wear resistance, good chemical inertness, good thermal and electrical conductivity zirconium diboride (ZrB_2) can be a better choice to prepare PAMCs for high temperature applications[12,13]. Moreover, ZrB_2 also has the potential to replace Al_2O_3 and SiC in many applications[14,15].

Several workers have studied different systems for high temperature applications to see the effect of temperature on strength retention due to reinforcement. Sahoo and Koczak[16], prepared Al-4.5wt.%Cu/TiC *insitu* composites and studied the tensile properties at elevated temperature. They observed that yield strength and tensile strength of composites were improved by 130% and 65% respectively when compared with Al-4.5wt. % Cu matrix alloy processed in the similar conditions. They also observed that composite was able to retain its room temperature strength up to 250°C. Lee et al.[17] investigated the effects of temperature and strain rate on flow properties of carbon-fiber-reinforced 7075 aluminium alloy metal-matrix composite and concluded that flow stress increases with strain rate, but decreases with temperature. Work-hardening rates decrease with increasing strain and temperature. Hoseini and Meratian[18] studied the tensile properties of *insitu* aluminium alumina composites at ambient as well as at high temperature. They observed that effect of alloying elements on strengthening was more

*e-mail: narendra.dharwan@gmail.com

significant at room temperature as compared to composite reinforced with 5 wt.% alumina particles. Whereas, at high temperature (300°C) tensile strength is largely controlled by reinforcement and composite has higher strength due to strain- hardening effect of alumina particles, while alloying elements lose their strengthening effect at high temperature. Yi et al.[19] studied the high temperature mechanical properties of *insitu* TiB_{2p} reinforced Al-Si alloy composites and reported that tensile strength of composites were higher than Al-Si master alloy at temperatures ranging from 25° to 400°C. Oñoro[20] studied high temperatures mechanical properties of TiB_2 particles reinforced AMCs based on aluminium alloys (6061 and 7015) up to 500°C. The tensile strengths of the AMCs and the aluminium alloys decreased as the temperature increased, but the ductility was found to increase. Han et al.[21] also investigated the tensile behaviour and fracture mechanism of Al-12Si/4 wt. % TiB_2 composite in a temperature range of 25° to 350°C and observed the improvement in elastic modulus of composites as compared to matrix alloy. At ambient temperature the composite exhibits more yield and tensile strength than unreinforced alloy. However at 200°C and 350°C no significant difference in the strength of composite and alloy was observed. The ductility of the composite was found to be lower than that of the unreinforced matrix alloy at 25° and 200°C, but no major difference was observed at 350°C. Morphology of the fractured surface of Al-Si /TiB_2 composite showed that at 25° and 200°C, the fracture mechanism was dominated by cracking of silicon particles and separated TiB_2 particles. Whereas, de-bonding of the silicon particles coupled with failure of the interface between TiB_2 particles and matrix were the dominant fracture mechanisms at 350°C. Recently, Ram et al.[22] investigated high temperature tensile properties of centrifugally cast in-situ Al-Mg_2Si functionally graded composites and observed the reduction in strength with increase in temperature. Fracture mode was changed from mixed mode to ductile mode at high temperature.

There is lack of information on the high temperatures tensile behaviour of PAMCs reinforced with nanosize or submicron particles. El-Kady et al.[23] investigated; the tensile properties of A356/Al_2O_3 nanocomposites at both ambient and elevated temperature. Tensile results revealed that nanocomposites exhibited better mechanical properties than the unreinforced alloy at both ambient and elevated temperatures up to 300°C. Moreover, with increased amount and reduced size of Al_2O_3 particles both tensile and yield strength was observed to be increased. The information related high temperature strength is very important where nanosize PAMCs are being considered as candidates to replace steel or aluminium alloys for piston liners and cylindrical heads of automobile engines, as well as brake rotors which are used for high temperature industrial applications. Hence, present study is focussed on high-temperature tensile and strain hardening behaviour of AA5052/ 9 vol. % ZrB_2 composite. Further, tensile results are correlated with morphology of fractured surface to understand the mechanism of failure at elevated temperature.

2. Experimental Details

2.1 Raw material, and synthesis of composite

AA5052 aluminium alloy (Al-2.5Mg-0.2Cr) was received from Hindalco Industries, Renukoot, India and two inorganic salts K_2ZrF_6 and KBF_4 were purchased from Sigma Aldrich, Bangalore, India. Casting was done on stir casting furnace with bottom pouring arrangement. AA5052 alloy has been reinforced with 9 vol. % ZrB_2 particles by *insitu* synthesis. Detailed procedure for preparing the Al/ZrB_2 composite by *insitu* synthesis has been discussed in our earlier published work[24]. Fig.1 shows flow chart for synthesizing the composite. Casting ingots were cut and machined to prepare the samples for various characterizations.

2.2 Characterization equipment

In order to confirm the formation of ZrB_2 particles XRD (Rigaku, CuK_α radiation of wavelength 1.541836 Å) study was carried out. Matrix grain size, morphology and distribution of ZrB_2 particle in the matrix were examined under Optical Microscope (Leitz Metallux-3) and Scanning Electron Microscope (FESEM Quanta 200FEG) respectively. Cylindrical specimens for high temperature tensile testing were prepared according to BS 12-1950 British standards (gauge diameter, 4.5 mm, gauge length, 15.5 mm) and tested on a computerized 100 kN screw-driven Instron™ Universal Testing Machine (model 4206) at temperatures ranging from room temperature (RT) to 200°C at a constant strain rate of 1.07/ 10^{-3} s^{-1}. Three specimens for each composition were tested at different temperatures and average values are reported. Fractured surface were examined under SEM to understand the failure mechanism at high temperature and correlated with the properties.

3. Results and Discussion

3.1 X-ray diffraction (XRD) study

During the composite synthesis *insitu* reaction takes place between the molten alloy and salts K_2ZrF_6 and KBF_4 at 860ºC according to following reactions[3,25].

$$K_2ZrF_6 + \frac{13}{3}Al = Al_3Zr + \frac{4}{3}AlF_3 + 2KF \quad (1)$$

$$2KBF_4 + 3Al = AlB_2 + 2AlF_3 + 2KF \quad (2)$$

$$Al_3Zr + AlB_2 = ZrB_2 + 4Al \quad (3)$$

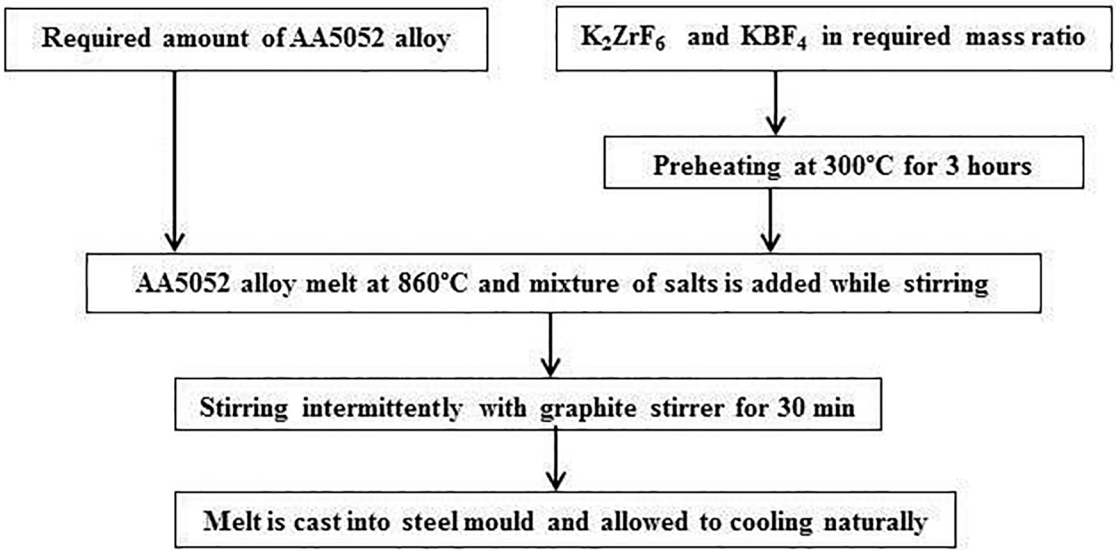

Figure 1. Flow chart for synthesizing the composite.

XRD pattern of synthesized materials with 0 and 9 vol. % ZrB_2 particles are shown in Fig.2a. Diffraction peaks of ZrB_2 particles are the sign of formation of ZrB_2 particle in the matrix by *insitu* reaction. For the secondary confirmation, ZrB_2 particles were extracted from the composite sample by dissolving small chips of composite in 10% HCl solution for several days and filtered. Filtered residue was thoroughly washed, dried and examined under XRD machine. Figure 2b shows the XRD pattern of extracted particles in which ZrB_2 peaks can be clearly seen.

3.2 Microstructural study

Optical micrographs of aluminium alloy and composite materials are shown in Fig. 3 a-b respectively[26]. Aluminium grains were refined due to *insitu* formed ZrB_2 particles. Grain size was measured with linear intercept method and found to be 115 µm for alloy and 67 µm for composite material respectively[10]. *Insitu* formed ZrB_2 particles restrict the growth of Al-rich grains during solidification process which results in refined grain structure[27]. ZrB_2 particle morphology and distribution are examined under SEM. Figure 4 a-b shows SEM micrographs of alloy and composite material. Fig. 4b shows that ZrB_2 particles are uniformly distributed in the matrix[24]; however, particles are agglomerated at some places due to their finer size. ZrB_2 particles are observed in hexagonal and rectangular morphology as shown in Fig. 4 c.

Reprinted from Kumar N. et al., 2015. Wear and friction behaviour of in-situ AA5052/ZrB_2 composites under dry sliding condition, Tribology in Industry, 37(2) 244-256, with permission from Faculty of Engineering[26].

Fig. 4b, Reprinted from Kumar N. et al., 2015. In-situ development of ZrB_2 particles and their effect on microstructure and mechanical properties of AA5052 metal-

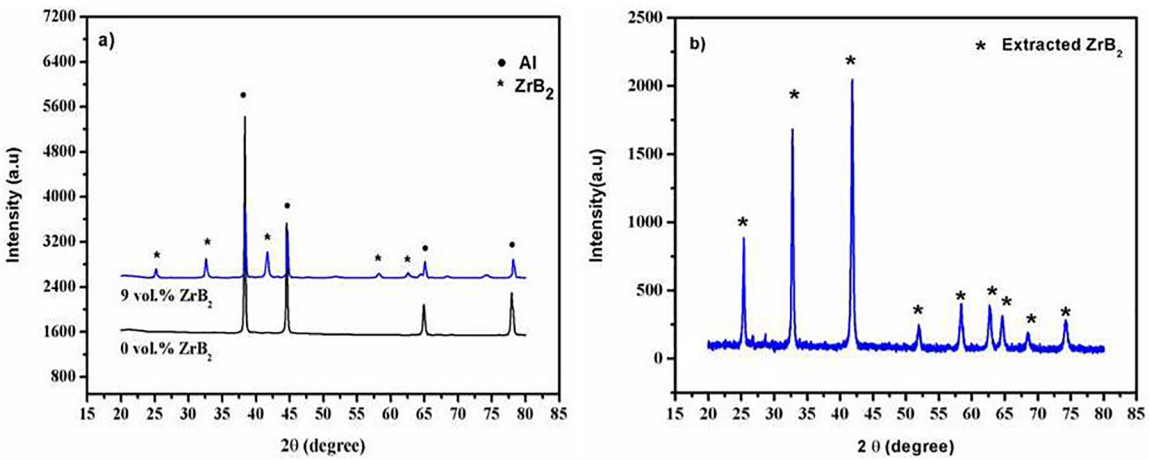

Figure 2. XRD pattern of (a) 0 and 9 vol. % ZrB_2 composite (b) extracted particle of ZrB_2.

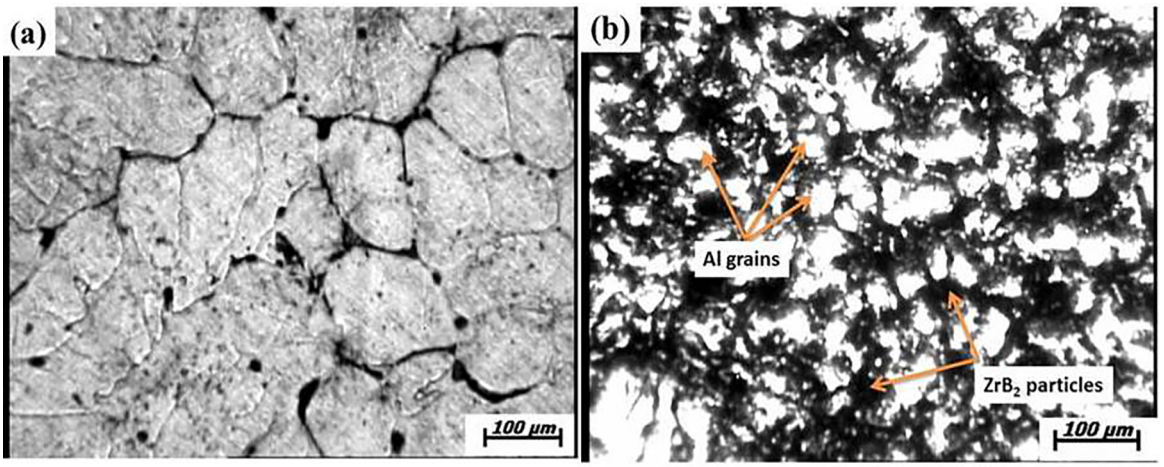

Figure 3. Optical micrograph of (a) alloy with 0 vol. % ZrB_2 (b) composite with 9 vol. % ZrB_2.

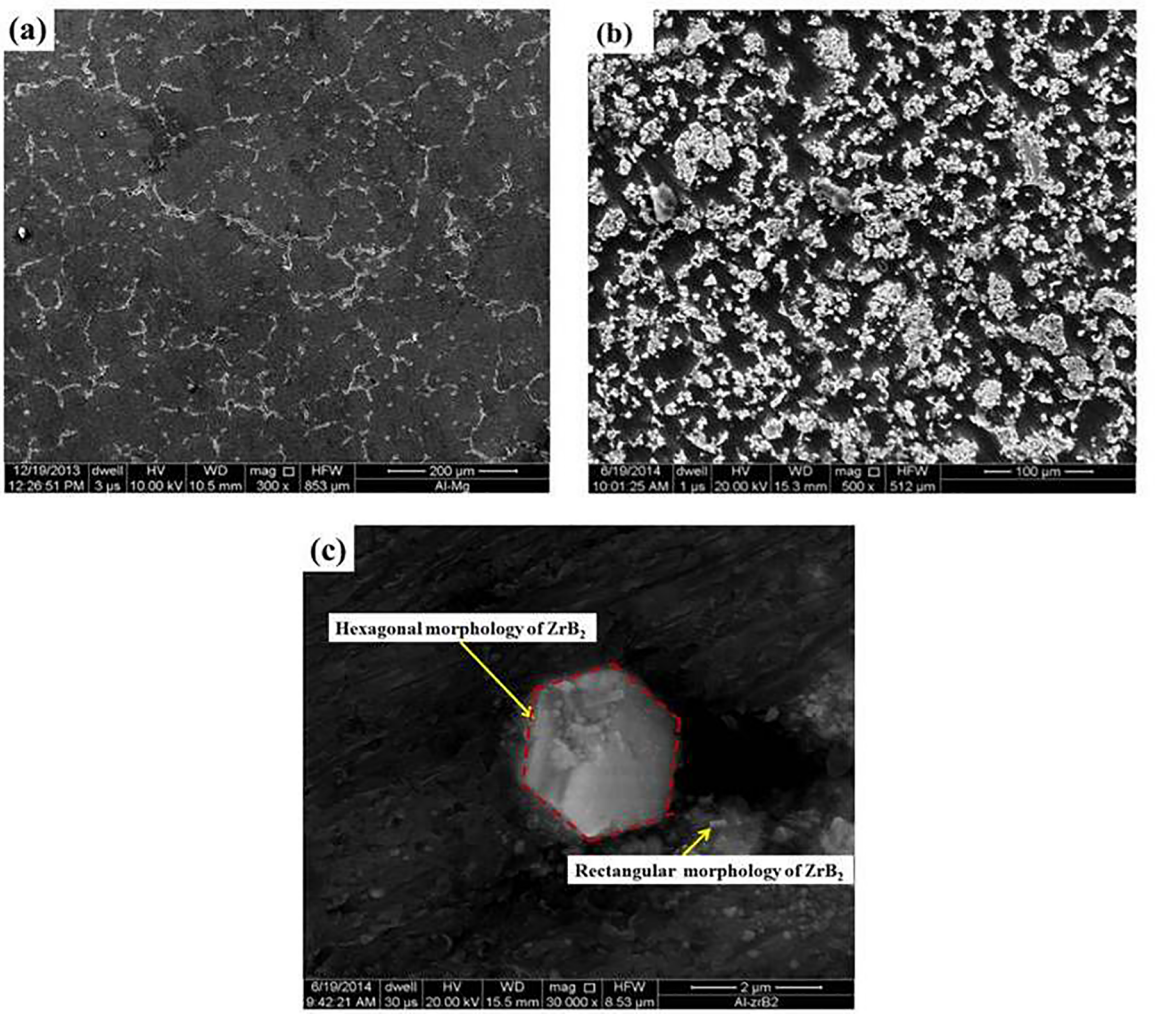

Figure 4. SEM micrograph of (a) alloy with 0 vol. % ZrB_2 (b) composite with 9 vol. % ZrB_2 (c) ZrB_2 morphology at high magnification.

matrix composites. Materials & Design,*80*, pp. 129-136 with permission from Elsevier[24]

3.3 High temperature tensile behaviour

Tensile tests for composites were conducted at an interval of 50°C up to a temperature of 200°C at a strain rate of 1.07 / 10^{-3} s^{-1}. Figure 5 a-c shows the variation of UTS, YS and percentage elongation with temperature for 9 vol. % ZrB_2 composite. The Experimental results reveal that UTS and YS of composite decrease linearly with increase in operating temperature. Composite exhibits good resistance to high temperature effects in terms of strength. Even at 150°C the UTS of composite is 81% of the ambient temperature strength, and at 200°C also 72% of the ambient temperature strength is retained. It should also be noted that percentage elongation (ductility) increases as the test temperature increases due to thermal softening of the matrix.

3.4 High temperature strain hardening behaviour

Influence of ZrB_2 particles on tensile strength at high temperature can be studied in terms of strain hardening. Beyond macroscopic yield, strain hardening behaviour of composite is described by power law which is given by $\sigma = K\varepsilon_p^{n}$[28], where σ and ε_ρ are the true stress and true plastic strain respectively. Figure 6a shows true stress (σ) and true plastic strain (ε_ρ) curve on log-log scale for composite at different temperatures 50ºC-200ºC. K is the monotonic strength coefficient (intercept at plastic strain (ε_ρ = 1) and n is strain hardening exponent representing slope of the curve. It is interesting to note in Fig. 6b that strain hardening exponent (n) is not significantly influenced by increasing the temperature, which is an indication of good strength retained by the composite even at high temperature. Similar kinds of results are also reported by other workers[29,30].

3.5 Fracture surface analysis

Fractured surface of composite with 9 vol. % ZrB_2 particles are shown in SEM micrographs (Figure 7 a-d). These figures correspond to tests conducted at RT, 100°, 150° and 200°C. The fractured surface morphology at high temperature is quite different from that of the room temperature. At room temperature the fractured surface clearly shows a large crack, initiated by high stresses due to the presence of large clusters of hard ZrB_2 particles as shown in Fig.7a. The major form of fracture, at room temperature, is the rupture of ZrB_2 particles from the matrix. Small size dimples are also seen

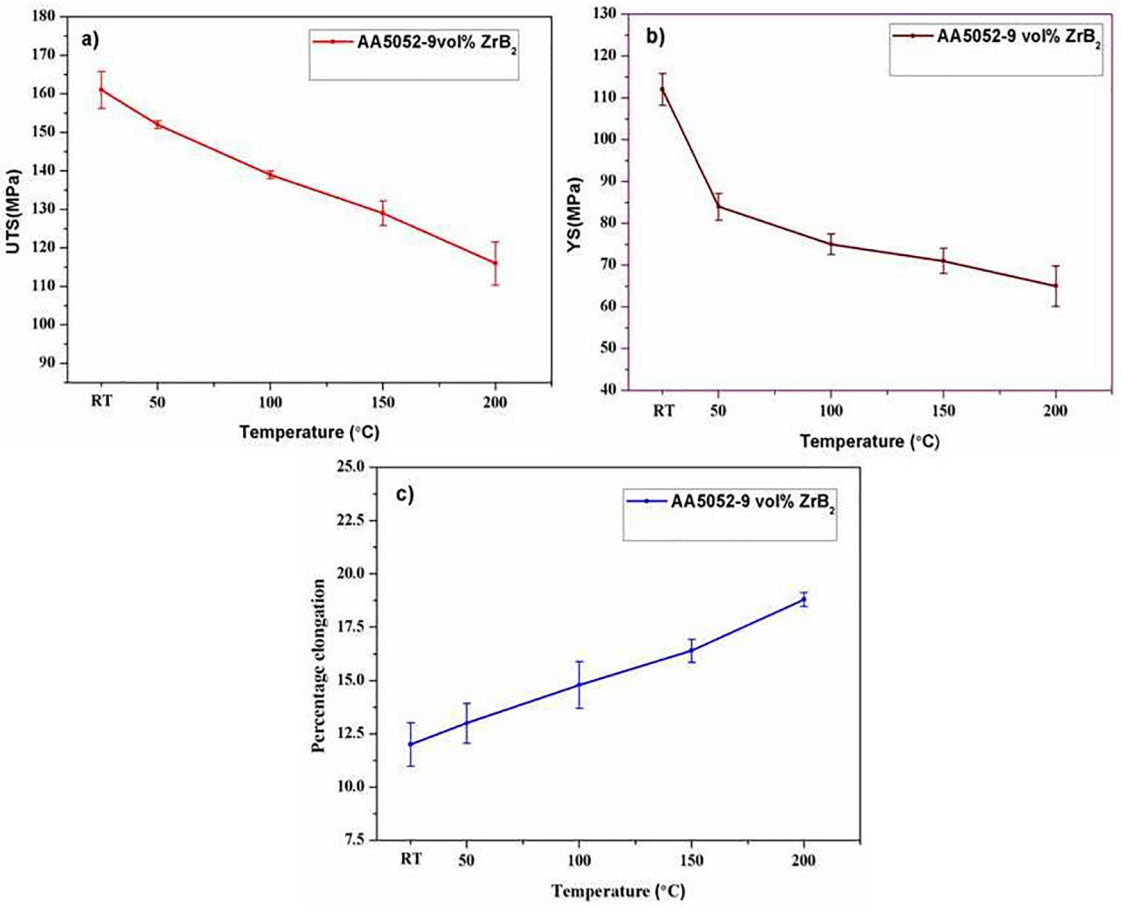

Figure 5. Variation of (a) UTS (b) YS and (c) percentage elongation with temperature.

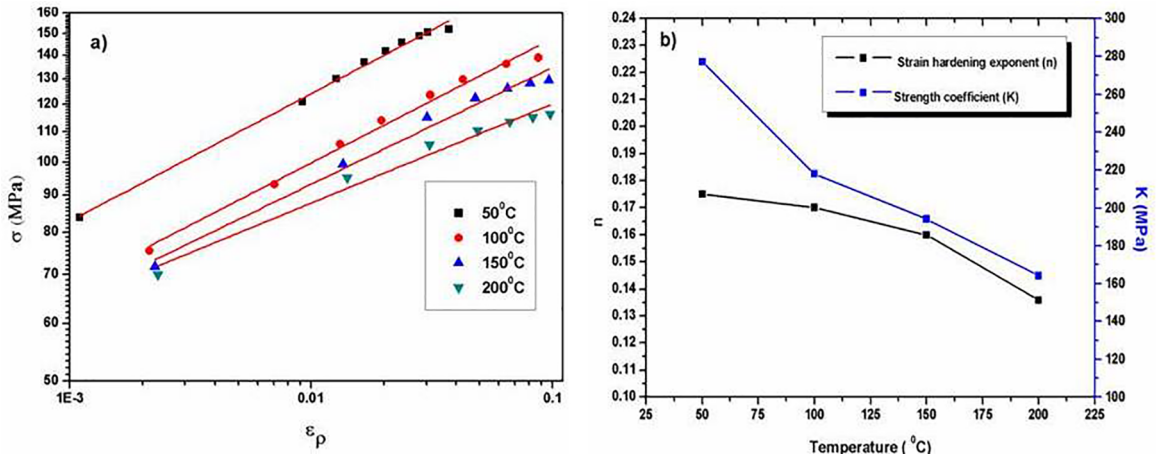

Figure 6. (a) log-log plot of σ vs. ε_ρ (b) variation of n and K with temperature.

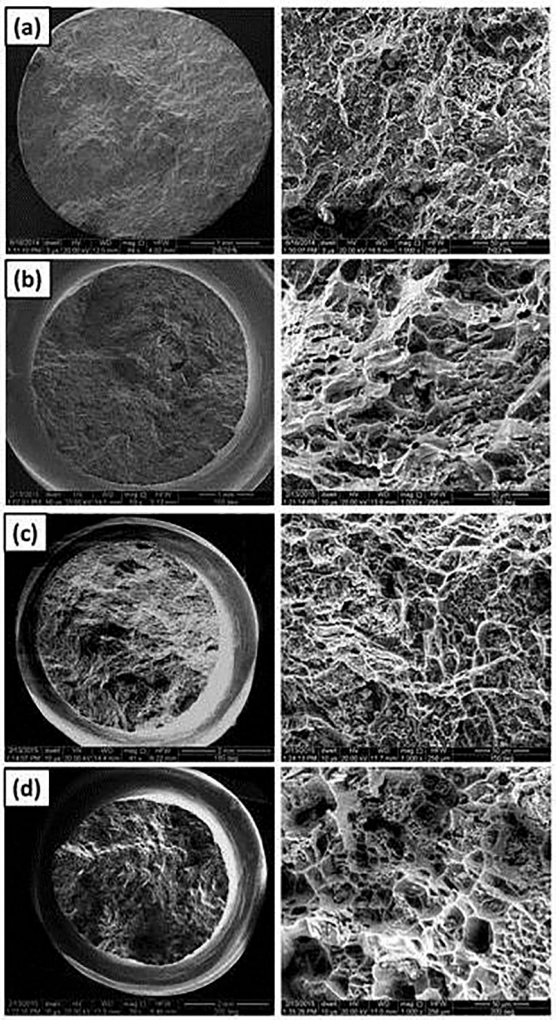

Figure 7. Fractographs of composite with 9 vol. % ZrB_2 at different temperatures (a) RT (b) 100°C (c) 150°C and (d) 200°C.

on the surface. With rise in temperature large size dimples of the matrix material along with large voids are seen on the surface. When the temperature reaches to 200°C (Fig.5.2d), thermal softening takes place and voids in the matrix act as dominant fracture mode, thereby, ductility is increased[18,20].

4. Conclusion

From present study following conclusions can be drawn:

1. Reinforced ZrB_2 particles are confirmed by XRD analysis which indicate successful synthesis of AA5052/9vol. % ZrB_2 composite by *insitu* technique with hexagonal and rectangular ZrB_2 particles with uniform distribution in the matrix.
2. UTS and YS of composite decrease with increasing the temperature, while the ductility shows opposite trend.
3. Composite retains its 81% of ambient temperature UTS at 150°C and 72% at 200°C.
4. Temperature has very little effect on the strain hardening exponent, which shows the strain hardening capability of composite at high temperature.
5. Fractured surface morphology is very well in agreement with tensile results.

5. References

1. Deuis RL, Subramanian C, Yellup JM. Dry sliding wear of aluminium composites-A review. *Composites Science and Technology*. 1997;57(4):415-435.

2. Zhang SL, Zhao YT, Chen G, Cheng XN, Huo XY. Fabrication and dry sliding wear behaviour of in situ Al-K_2ZrF_6-KBF_4 composites reinforced by Al3Zr and ZrB_2 particles. *Journal of Alloys and Compounds*. 2008;450(1-2):185-192.

3. Dinaharan I, Murugan N, Parameswaran S. Influence of in situ formed ZrB_2 particles on microstructure and mechanical properties of AA6061 metal matrix composites. *Materials Science and Engineering: A*. 2011;528(18):5733-5740.

4. Gautam G, Mohan A. Effect of ZrB2 particles on the microstructure and mechanical properties of hybrid ($ZrB_2 + Al_3Zr$)/AA5052 insitu composites. *Journal of Alloys and Compounds*. 2015;649:174-183.

5. Mohan A, Gautam G, Kumar N, Mohan S, Gautam RKC. Synthesis and tribological properties of AA5052-base insitu composites. *Composite Interfaces*. 2016;23(6):503-518.

6. Kumar N, Gautam G, Gautam RK, Mohan A, Mohan S. High-Temperature Tribology of AA5052/ZrB_2 PAMCs. *Journal of Tribology*. 2017;139(1):011601.

7. Tee KL, Lu L, Lai MO. Synthesis of in situ Al-TiB_2 composites using stir cast route. *Composite Structures*. 1999;47(1-4):589-593.

8. Sahin Y. Preparation and some properties of SiC particle reinforced aluminium alloy composites. *Materials & Design*. 2003;24(8):671-679.

9. Wang H, Li G, Zhao Y, Chen G. In situ fabrication and microstructure of Al_2O_3 particles reinforced aluminum matrix composites. *Materials Science and Engineering: A*. 2010;527(12):2881-2885.

10. Kumar N, Gautam G, Gautam RK, Mohan A, Mohan S. A study on Mechanical Properties and Strengthening Mechanisms of AA5052/ZrB_2 in Situ Composites. *Journal of Engineering Materials and Technology*. 2017;139(1):011002.

11. Lee KB, Sim HS, Heo SW, Yoo HR, Cho SY, Kwon H. Tensile properties and microstructures of Al composite reinforced with BN particles. *Composites Part A: Applied Science and Manufacturing*. 2002;33(5):709-715.

12. Zhang X, Xu L, Du S, Han J, Hu P, Han W. Fabrication and mechanical properties of ZrB_2-SiCw ceramic matrix composite. *Materials Letters*. 2008;62(6-7):1058-1060.

13. Zhang X, Luo X, Li J, Han J, Han W, Hong C. Structure and bonding features of ZrB_2 (0 0 0 1) surface. *Computational Materials Science*. 2009;46(1):1-6.

14. Sonber JK, Murthy TSR, Subramanian C, Kumar S, Fotedar RK, Suri AK. Investigations on synthesis of ZrB_2 and development of new composites with HfB_2 and $TiSi_2$. *International Journal of Refractory Metals and Hard Materials*. 2011;29(1):21-30.

15. Guo SQ, Kagawa Y, Nishimura T. Mechanical behavior of two-step hot-pressed ZrB_2-based composites with $ZrSi_2$. *Journal of the European Ceramic Society*. 2009;29(4):787-794.

16. Sahoo P, Koczak MJ. Microstructure-property relationships of in situ reacted TiC/Al-Cu metal matrix composites. *Materials Science and Engineering: A*. 1991;131(1):69-76.

17. Lee WS, Sue WC, Lin CF. The effects of temperature and strain rate on the properties of carbon-fiber-reinforced 7075 aluminium alloy metal-matrix composite. *Composites Science and Technology*. 2000;60(10):1975-1983.

18. Hoseini M, Meratian M. Tensile properties of in-situ aluminium-alumina composites. *Materials Letters*. 2005;59(27):3414-3418.

19. Yi H, Ma N, Li X, Zhang Y, Wang H. High-temperature mechanics properties of in situ TiB_2p reinforced Al-Si alloy composites. *Materials Science and Engineering: A*. 2006;419(1-2):12-17.

20. Oñoro J. High-temperature mechanical properties of aluminium alloys reinforced with titanium diboride (TiB_2) particles. *Rare Metals*. 2011;30(2):200-205.

21. Han G, Zhang W, Zhang G, Feng Z, Wang Y. High-temperature mechanical properties and fracture mechanisms of Al-Si piston alloy reinforced with in situ TiB_2 particles. *Materials Science and Engineering: A*. 2015;633:161-168.

22. Ram SC, Chattopadhyay K, Chakrabarty I. High temperature tensile properties of centrifugally cast in-situ Al-Mg_2Si functionally graded composites for automotive cylinder block liners. *Journal of Alloys and Compounds*. 2017;724:84-97.

23. El-Kady ES, Mahmoud TS, Sayed MA. Elevated Temperatures Tensile Characteristics of Cast A356/Al_2O_3 Nanocomposites Fabricated Using a Combination of Rheocasting and Squeeze Casting Techniques. *Materials Sciences and Applications*. 2011;2(5):390-398.

24. Kumar N, Gautam RK, Mohan S. In-situ development of ZrB_2 particles and their effect on microstructure and mechanical properties of AA5052 metal-matrix composites. *Materials & Design*. 2015;80:129-136.

25. Tian K, Zhao Y, Jiao L, Zhang S, Zhang Z, Wu X. Effects of in situ generated ZrB_2 nano-particles on microstructure and tensile properties of 2024Al matrix composites. *Journal of Alloys and Compounds*. 2014;594:1-6.

26. Kumar N, Gautam RK, Mohan S. Wear and Friction Behavior of in-situ AA5052/ZrB_2 Composites under Dry Sliding Conditions. *Tribology in Industry*. 2015;37(2):244-256.

27. Rohatgi P, Gupta N, Schultz B, Daoud A. *Solidification during casting of metal-matrix composites*. In: ASM Handbook. Volume 15: Casting. Materials Park: ASM International; 2013. p. 390-397.

28. Hollomon JH. Tensile deformation. *Transactions of the Metallurgical Society of AIME*. 1945;12:268-290.

29. Srivatsan TS, Al-Hajri M, Smith C, Petraroli M. The tensile response and fracture behavior of 2009 aluminum alloy metal matrix composite. *Materials Science and Engineering: A*. 2003;346(1-2):91-100.

30. Srivatsan TS. Microstructure, tensile properties and fracture behaviour of Al2O3 particulate-reinforced aluminium alloy metal matrix composites. *Journal of Materials Science*. 1996;31(5):1375-1388.